Broad-Band Chiral Reflectors based on Nano-Structured Biological Materials

D.J. Brink, N.G. van der Berg, L.C. Prinsloo, and A. Botha

Abstract—In this work we study the reflection of circularly polarised light from a nano-structured biological material found in the exocuticle of scarabus beetles. This material is made of a stack of ultra-thin (~5 nm) uniaxial layers arranged in a left-handed helicoidal stack, which resonantly reflects circularly polarized light. A chirp in the layer thickness combined with a finite absorption coefficient produce a broad smooth reflectance spectrum. By comparing model calculations and electron microscopy with measured spectra we can explain our observations and quantify most relevant structural parameters.

Keywords—Chiral reflectors, circularly polarised light, helicoidal structures, nano photonics.

I. INTRODUCTION

NANO-STRUCTURED materials exhibiting interesting and useful photonic features are not limited to modern science and technology. Biological materials with photonic crystal properties can also be found in the animal kingdom. A typical example is the helicoidal stack [1] of ultra thin (~ 5 nm) layers comprising the exocuticle of several brightly coloured scarabus beetle species. Usually these materials are excellent narrow-band reflectors [2, 3, 4, 5, 6] for (left) circularly polarized light whenever the pitch of the helix associated with the circularly polarized light wave matches the pitch of a helicoidally arranged thin film stack [1].

In this study of the optical and structural properties of the beetle *Gymnopleurus humanus,* using visible reflectance measurements combined with electron microscopy, we noticed that the exocuticle of this beetle differs somewhat from that of previously investigated specimens in that the material is slightly absorbing instead of completely transparent and, in addition, the layer thickness shows a distinct chirp. Computer modelling shows that the combination of these two effects substantially widens the spectral width of the observed reflection peak.

In this work we represent a detailed characterisation and explanation of these biological broad-band chiral reflectors and show how absorbing and chirped structures can be modelled. We believe that they can also find practical applications in the fabrication of nano-engineered chiral reflectors and filters used in displays and laser technology.

The authors are with the Department of Physics, University of Pretoria, Pretoria 0002, South Africa.
Corrsponding author: D.J. Brink, johan.brink@up.ac.za, TEL +27(0)1245203502, FAX: +27(0)123625288.

II. THEORY

In most scarabus beetles the exocuticle is comprised of a stack of ultra-thin layers, each made up of a large number of micro fibrils all oriented in the same way[1]. Light polarised along the fibrils then experience a slightly larger index of refraction and the layer acts as a uniaxial medium with indices of refraction $n_1 > n_2$ along and perpendicular to the fibrils. It is useful to express these as:

$$n_1 = \frac{n_{av} + \delta n}{2} \quad \text{and} \quad n_2 = \frac{n_{av} - \delta n}{2} \quad , \qquad (1)$$

where δn is the birefringence of the material and n_{av} is the average index of refraction, which can be directly measured as shown below. For an absorbing material a complex index of refraction should be used:

$$N_{av} = n_{av} - k_e \quad , \qquad (2)$$

with k_e the extinction coefficient.

When each subsequent layer is rotated through a small angle relative to the layer above it, a helicoidal structure is obtained. Light propagation in such a stratified anisotropic medium can be modelled by using the Berreman matrix formulation [7, 8] of the Maxwell equations. For a structure stratified along the Z-axis and light incident along a plane of incidence parallel to the X-Z plane, propagation can be described by:

$$\frac{\partial \vec{\psi}}{\partial z} = -k_0 \bar{\bar{\Delta}} \vec{\psi} \quad , \qquad (3)$$

where $\vec{\psi}$ is a generalised field vector containing the four X- and Y-components of the electric and magnetic fields. $\bar{\bar{\Delta}}$ is the 4×4 Berreman propagation matrix:

$$\bar{\bar{\Delta}} = \begin{bmatrix} 0 & 1 - \dfrac{\eta^2}{\varepsilon_2 - i\varepsilon_i} & 0 & 0 \\ \varepsilon_{av} - i\varepsilon_i + \delta\varepsilon \cos\beta z & 0 & -\delta\varepsilon \sin\beta z & 0 \\ 0 & 0 & 0 & 1 \\ -\delta\varepsilon \sin\beta z & 0 & \varepsilon_{av} - i\varepsilon_i - \eta^2 - \delta\varepsilon \cos\beta z & 0 \end{bmatrix}$$

$$(4)$$

where ε_1 and ε_2 represent the dielectric constants along and perpendicular to the micro fibrils defined by $\varepsilon_1 = (n_{av} + \delta n / 2)^2$ and $\varepsilon_2 = (n_{av} - \delta n / 2)^2$, $\varepsilon_{av} = (\varepsilon_1 + \varepsilon_2)/2$ and $\delta\varepsilon = (\varepsilon_1 - \varepsilon_2)/2$. We modified the Berreman matrix to accommodate absorbing media by defining and incorporating an imaginary part of the dielectric

constant $\varepsilon_i = 2n_{av}k_e$. The other parameters in (4) are $\eta = n_0 \sin\phi_0$, with n_0 the ambient index of refraction and ϕ_0 the angle of incidence and $\beta = 2\pi/P_0$, with P_0 the pitch of the helicoidal structure.

In this work we tracked the spatial evolution of $\vec{\psi}$ by direct integration of (3):

$$\vec{\psi}(z+h) = e^{ik_0h\vec{\Delta}}\psi(z) \cong \vec{\tilde{L}}(h)\vec{\psi}(z) \ , \tag{5}$$

where h is the length of an integration step. Layer matrix $\vec{\tilde{L}}$ was calculated by a suitable series expansion (up to 9 terms) of the exponent [9]. The chirped nature of the layered structure was taken into account by increasing the value of P_0 after every integration step.

Azzam and Bashara [8] showed that the complex reflection matrix for the stratified structure :

$$\begin{bmatrix} r_{LL} & r_{LR} \\ r_{RL} & r_{RR} \end{bmatrix} , \tag{6}$$

can be calculated from the layer matrix. The elements represent the amplitude reflection coefficients for circularly polarized light (CPL). Terms r_{LL} and r_{RR} give reflection for left incident and reflected CPL as well as right incident and reflected CPL, respectively. The cross terms give reflection coefficients where the rotation sense is inverted after reflection. A normal mirror reflection gives only these off-diagonal terms. Helicoidal structures give non-zero diagonal terms.

Whenever the helix associated with the light match the helix of the layered structure optimum reflection is obtained:

$$\lambda = n_{av}P_0 \cos\phi_1 \ , \tag{7}$$

where ϕ_1 is the propagation direction of the light in the stratified medium relative to the Z-axis. This is just a modified version of the well known Bragg condition for thin-film interference.

III. EXPERIMENTAL

Gymnopleurus. humanus beetles are not nearly as bright as the *Gymnopleurus virens* specimens studied earlier [2, 3], which indicates that their exocuticles are absorbing. They are found in many different colours depending on the region they live in [10]. Three representative specimens (blue-green (A), yellow-green (B) and red (C)) were chosen for this research. Samples were cut from the thorax of the specimens as sufficiently flat and smooth regions could be found here to allow reproducible quantitative work.

Reflection spectra were recorded by illuminating samples with a collimated beam of white light from a tungsten-halogen lamp. Both input and reflected beams were passed through circular polarisers and then analysed with a 0.6m monochromator from Jobin Yvon. All spectra were normalised by dividing point by point with the spectrum of the light source, which compensates for the spectral response of the measuring instrument as well as for the spectral distribution of the source. Spectra were recorded for a range

in incident angles to allow calculation of n_{av} as well as P_0 according to the procedure outlined in section IV B.

An attempt was made to estimate absolute reflection values by comparing the measured LR reflectance to calculated values. These mirror-like reflections are very insensitive to the details of the helicoidal structure and depend mainly on n_{av}, which can be measured directly (section IV B). For perpendicular incidence :

$$R_{LR} = (r_{LR})(r_{LR})^* \cong \left(\frac{n_{av}-1}{n_{av}+1}\right)^2 . \tag{8}$$

R_{LR} can be measured by rotating the final quarter-wave plate through 90° compared to the setup for measuring R_{LL} allowing a simple in-line comparison of values.

Scanning electron microscopy (SEM) work was performed with a Zeiss ultra plus ultra-high resolution FEG SEM instrument using secondary electron imaging. During recordings the sample was tilted by an angle of 30° with respect to the incoming electron beam to enhance the visibility of the edges of the layered structure. Darker and lighter parts represent a 180° rotation (half a pitch length) of the microfibrils.

IV. RESULTS AND DISCUSSION

A. Electron microscopy

A scanning electron microscope (SEM) picture of a cross section of the exocuticle of the yellow-green beetle (B) is shown in Fig.1.
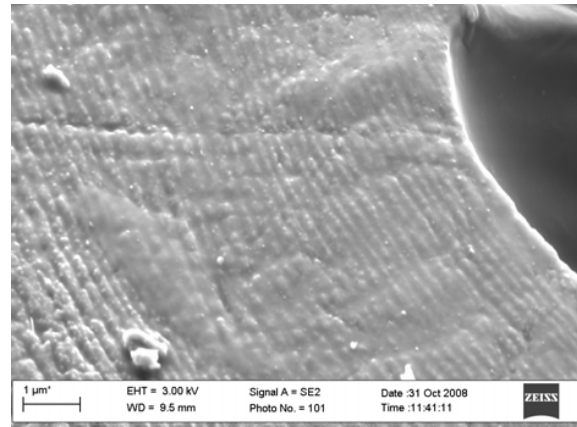

Fig. 1 SEM micrograph of a cross section of the exocuticle of beetle B. One light-dark cycle represents half a pitch length.

As explained in earlier work [1, 2] the layers shown in SEM micrographs represent a half pitch (distance over which the fibrils rotate through 180°) of the layered structure. In Fig. 1 this is about $0.19\ \mu m$ close to the surface. According to the Bragg condition (7), this should produce a reflectance peak at $\lambda = n_{av}P_o \cong 570\ nm$ (see section IV B) for near normal incidence. A closer inspection of the layer spacing reveals

that there is a definite chirp in layer thickness to larger values deeper into the exocuticle, but it is hard to quantify this for the first few layers, which are most important in determining the position of the reflection peak. It does, however, qualitatively explain the difference between the observed peak position at 580 nm and its predicted position. Similar results were obtained for beetles A and C where half pitch values of approximately 0.17 μm and 0.22 μm were obtained.

B. Measurement of n_{av} and P_0

According to the Bragg condition (7) the reflectance peak should shift to the blue with increasing angle of incidence. By relating the internal propagation angle ϕ_1 to the external angle of incidence ϕ_0 via Snell's law: $n_0 \sin\phi_0 = n_1 \sin\phi_1$ condition (7) changes to:

$$\sin^2 \phi_1 = -\frac{1}{P_0}\lambda^2 + n_{av}^2 \qquad (9)$$

By fitting a straight line to a plot of experimentally observed peak wavelength squared versus the sine of the angle of incidence squared independent values can be obtained for average index of refraction as well as the average pitch length (distance over which the orientation of the micro fibrils rotates through 360°). If the pitch increases with depth due a chirp in layer thickness, P_0 will be an average over all layers participating in the reflection process and this in turn depends on the absorption coefficient of the material. Hence the interpretation of the P_0 value is still somewhat ambiguous at this stage.
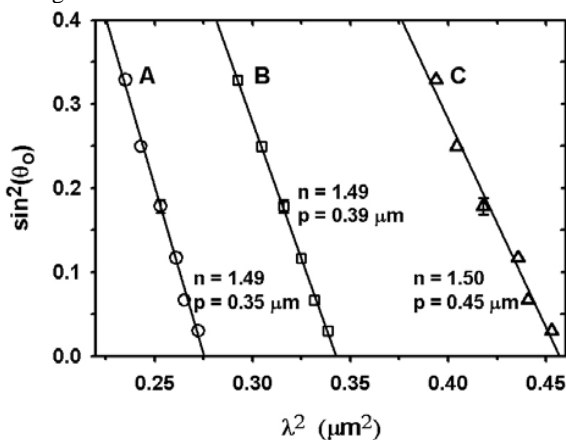
Fig. 2 Dependence of peak wavelength on angle of incidence of samples A, B and C. Extrapolated values of index of refraction and pitch length are shown.

Fig. 2 shows the results for the three beetles studied in this work. Within experimental error the refractive index $n_{av} = 1.49 \pm 0.02$ is the same for all three samples. This is somewhat lower than the value of 1.61 obtained for *Gymnopleurus virens* in earlier work and indicates that the exocuticle of *Gymnopleurus humanus* is possibly more porous.

The full pitch values obtained for beetles A, B and C were 0.35, 0.39 and 0.45 μm respectively with an estimated error of about $\pm 0.01\mu$m. These are in reasonable agreement with the SEM micrographs, especially if the presence of a thickness chirp is taken into account.

C. Reflection Spectra

In this section we show that it is possible obtain estimated values for all structural parameters determining the optical properties of the nano-structured exocuticle of humanus beetles, by comparing observed and modelled reflectance spectra.
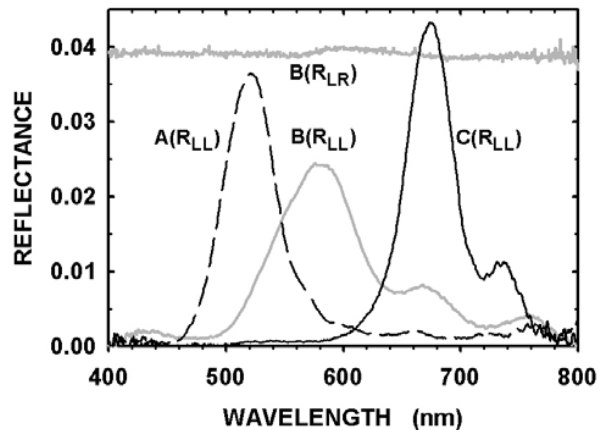
Fig. 3 Experimentally measured reflectance spectra at an angle of incidence of 10°.

Experimental reflectance spectra for beetles A, B and C are shown in Fig. 3. It is immediately evident that peak reflectance values are rather low. Even for resonant R_{LL} reflections best values are in the order of 4% in spite of the fact that the SEM micrographs show that over 20 pitch lengths are available for resonant Bragg scattering. This is a clear indication that the exocuticle material has to be absorbing. Absorption, represented by the extinction coefficient k_e, limits the number of pitch-lengths involved in the scattering process and as with any multi-layer interference phenomenon this drops and broadens the reflection peak.

This is illustrated in Fig. 4 which shows the influence of an increasing k_e value on the height and width of the main reflectance peak according to a model based on the theory in section II. For sample B, exhibiting the lowest and widest peak a k_e value of 0.045 in Fig.4 produces a calculated refection peak of about 2%, which is slightly below the observed maximum. One can therefore consider this as an upper limit for k_e.

At this k_e value the predicted FWHM (full width at half maximum) is around 38 nm which is much smaller than the observed value of 84 nm.
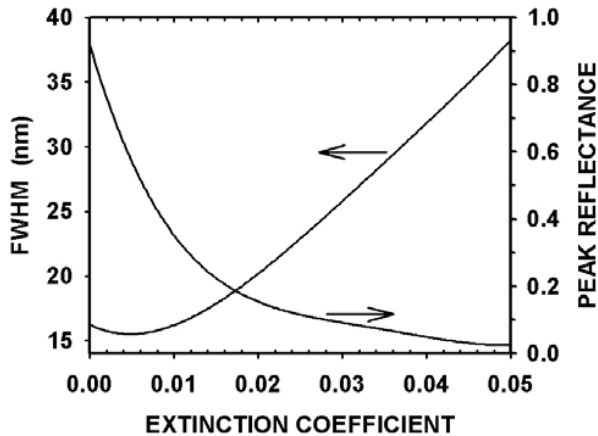
Fig. 4 Calculated dependence of the width and height of the
main reflectance peak on extinction coefficient for
sample B.

It is therefore evident that absorption alone cannot explain the
width of the peak and some amount of chirp in the pitch
length is required to obtain the observed width. As shown in
Fig. 5 the presence of even a very small amount of chirp
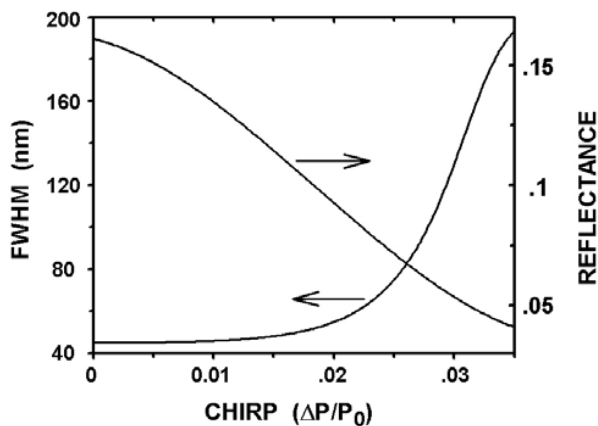($\Delta P / P_0$) can significantly broaden the reflectance peak.

Fig. 5 Calculated dependence of the width and height of the
main reflectance peak on chirp for sample B.

As can be expected the number of pitch lengths (N_0) involved
in the reflection process play a key role in the total amount of
chirp and therefore also in the amount of induced broadening.
This number of pitch lengths, in turn, is determined by the
absorption coefficient. For a k_e value of around 0.035 the
incident light intensity drops to ~20% over about 6 pitch
lengths, which is therefore a useful estimate for N_0. For this
N_0 value the expected FWHM (without any absorption) is
obtained for a chirp of $\Delta P / P_0 \cong 0.025$, which can then be
regarded as an upper limit for chirp.

If we now assume that the exocuticle material itself is the
same for all humanus beetles all three specimens should have
approximately the same values for n_{av}, δn and k_e. This view
is supported by the observation that the reflectance spectra for
non-resonant mirror-like reflections (R_{LR}) are essentially flat.

Applying this restriction and by comparing the width, height
and position of the main reflectance peaks for all three
specimens investigated, it is possible to obtain a unique
solution for these parameters as well as for the pitch P_0 and
the chirp $\Delta P / P_0$. Best-fit parameter values are listed in Table
I.

TABLE I
BEST-FIT VALUES FOR MODEL PARAMETERS

parameter	A	B	C
λ_0 (nm)	521	580	674
P_0 (μm)	0.332	0.357	0.442
$\Delta P / P_0$	0.0093	0.022	0.0036
n_{av}	1.49	1.49	1.49
δn	0.035	0.035	0.035
k_e	0.034	0.034	0.034

It should be noted that the P_0 values listed in Table I refer
to the pitch length of the very first layer in the stack. If the
listed chirp is included and an average over six pitch lengths is
taken, reasonable agreement with the values in section IV B is
obtained.

A set of calculated reflectance spectra based on the best-fit
parameter values in Table I are shown in Fig. 6. A close
agreement with all the main features of the experimental
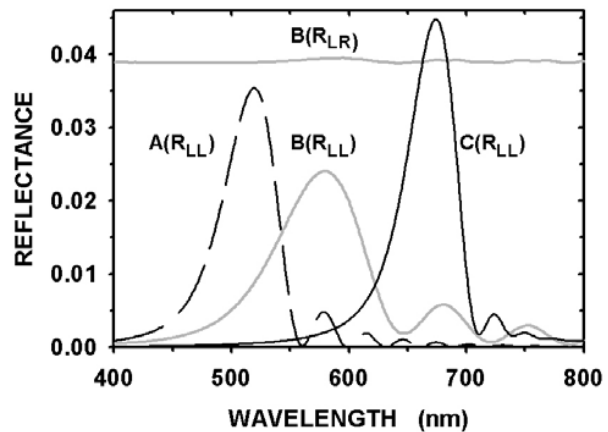spectra in Fig. 3 is obtained.

Fig. 6 Calculated reflection spectra based on the best-fit
parameter values in Table I

V. CONCLUSION

We have shown that the *Gymnopleurus humanus* beetle
employs a stack of nano-sized birefringent layers in its
exocuticle which generate resonant reflections of incident
circularly polarised light. Comparison with SEM micrographs
and model calculations show that a chirp in pitch length,
combined with a finite absorption coefficient, are responsible
for a considerable broadening of the reflectance spectrum.

This work may find practical applications in the fabrication of chiral reflectors used in display and laser technologies.

REFERENCES

[1] A.C. Neville and S. Caveney, "Scarab beetle exocuticle as an optical analogue of cholesteric liquid crystals" Biol. Rev., vol 44, pp. 531-568, 1969.

[2] D. J Brink, N. G. van der Berg, L. C. Prinsloo, and I.J. Hodgkinson, "Unusual coloration in scarabaeid beetles" J. Phys. D: Appl. Phys., vol 40, pp. 2189-2196, 2007.

[3] D. J Brink, N. G. van der Berg, and L. C. Prinsloo, "The role of interface effects on the reflection of circularly polarised light from the thin-film structure of scarabus beetles" Surf. Interface Anal., vol 40, pp. 769-771, 2008.

[4] I. Hodgkinson and Q. Wu, "inorganic chiral optical materials", Adv. Mater. vol 13, pp 889-897, 2001.

[5] K. M. Krause and M. J. Brett, "Spatially graded nanostructured chiral films as tunable circular polarizers", Ad. Funct. Mater., vol 18, pp. 3111-3118, 2008.

[6] D.H. Goldstein, "Polarization properties of scarabeidae" Appl. Opt., vol 45, pp. 7944-7950, 2006.

[7] D. W. Berreman, "Optics in stratified anisotropic media: 4X4-matrix formulation" J. Opt. Soc. Am., vol62, pp502-510, 1972.

[8] R. M. A. Azzam and N. M. Bashara, Ellipsometry and Polarized Light. Amsterdam: North Holland, 1989, pp 340-360.

[9] W. D. St John, W. J. Fritz, Z. J. Lu, and D. K. Yang, "Bragg reflection from cholesteric liquid crystals" Phys. Rev E, vol 51, pp. 1191-1198, 1995.

[10] A. L. V. Davis, D. J. Brink, C. H. Scholtz, L. C. Prinsloo, and C. M. Deshodt, "Functional implications of of temperature-correlated lolour polymorphism in an iridescent, scarabaeine dung beetle" Ecol.Entom., vol 33, pp. 771-779, 2008.